



# Growth and Characterization Studies of Potassium L-Alaninate NLO Single Crystal

Authors

**S. Anna Venus<sup>1</sup>, S.H. Mohammed Ameen<sup>2</sup>, R. Mary Jenila<sup>3</sup>, S. Anbarasu<sup>4</sup>  
Prem Anand Devarajan<sup>5\*</sup>**

<sup>1,3,4,5</sup>Physics Research Centre, Department of Physics, St. Xavier's College (Autonomous), Palayamkottai-627002, India

<sup>2</sup>Department of Physics, Sadakathullah Appa College, Rahmath Nagar, Palayamkottai-627002, India

\* Corresponding Author

**D. Prem Anand**

Assistant Professor of Physics

St. Xavier's College (Autonomous), Palayamkottai -627002, Tamilnadu, India.

Email: [dpremanand@yahoo.co.in](mailto:dpremanand@yahoo.co.in)

## Abstract

*Optical good quality defect free single crystals of Potassium L-alaninate (PLAla), was grown by slow evaporation technique at room temperature. The physico-chemical properties of the as grown crystals were analysed from single crystal XRD, thermal, spectral, and DC conductivity studies. From XRD analysis, it is assured that Potassium L-alaninate (PLAla), crystal belongs to orthorhombic system. A thermal study shows their endothermic response to heat. The melting point, average weight loss and possibility of phase transition and decomposition of the material were determined by TG-DTA analyses. The FTIR analysis confirms the functional groups present in the crystal. UV-Visible transmittance spectra was recorded to identify the transparency in visible and near infrared (NIR) region. The UV spectral studies show the good transparency of the crystals. The dielectric and AC conductivity studies were analysed as a function of resistance for various temperatures. The result reveals that the crystal of Potassium L-alaninate (PLAla) shows good AC electrical characteristics.*

**Key Words:** Potassium L-alaninate (PLAla), X-ray diffraction (XRD), Fourier transform infrared (FTIR), UV-vis-NIR, TG/DTA, Dielectric studies, AC conductivity, Micro Hardness and NLO properties.

## 1. INTRODUCTION

Second order nonlinear optical materials have recently attracted much attention because of their potential applications in emerging optoelectronic technologies <sup>[1]</sup>. Organic compounds are formed by weak Van der Waals and hydrogen bonds and possess a high degree of delocalization and they are optically more nonlinear than inorganic materials. Hence amino acids and their complexes have applications in NLO <sup>[2-4]</sup>. The importance of amino acids in NLO applications is due to the fact that all amino acids except glycine contain a chiral carbon atom and crystallize in

noncentrosymmetric space group. Therefore, they are efficient candidates for second harmonic generation, optical parametric amplifiers (OPA) and optical parametric oscillators (OPO). In addition, amino acids have peculiar physical and chemical properties due to the presence of a proton donor carboxyl acid (-COO) group and the proton acceptor amino group (NH<sub>2</sub>). In an amino acid, the carboxylic acid group donates its proton to the amino group to form a salt. Thus, in the solid, amino acid exists as a dipolar ion in which the carboxyl group is present as a carboxylate ion. Because of this dipolar nature, amino acids have properties that make them ideal candidates for

NLO applications. In view of these advantages, many works on characterization studies of L-alanine [5] and its related compounds L-alanine dimalic acid [6], L-alanine alaninium nitrate [7], L-alaninium fumarate [8], L-alanine acetate [9], L-alanine formate [10], L-alanine oxalate [11], Urea L-alanine acetate [12], L-alanine tetra fluoroborate [13] have been reported. The present work is focused on the growth and XRD, spectral, Thermal, microhardness, NLO and dielectric studies of Potassium L-alaninate (PLAla) for the first time.

## 2. MATERIALS AND METHODS

### 2.1 Synthesis

An appropriate stoichiometric amount of L-alanine and Potassium fluoride was taken with excess of doubly deionized water to synthesize PLAla. The reaction scheme is shown below. The as said reagents were dissolved in deionized water and saturated PLAla solution was prepared at room temperature. This saturated solution was placed in a constant temperature bath kept at the desired growth temperature.



### 2.2 Solubility

The solubility of pure PLAla in water was determined for five different temperatures 30, 35, 40, 45 and 50 °C respectively. Recrystallized salt was used for these studies. The solubility was determined by dissolving the solute in water, ethanol and methanol in an air tight container maintained at a constant temperature with continuous stirring. It was found that deionized water as the best solvent. After attaining saturation, equilibrium concentration of the solution was analyzed gravimetrically. The solubility curve for PLAla is shown in (Figure 1). It is seen from the solubility curve that PLAla increases with increase in temperature.

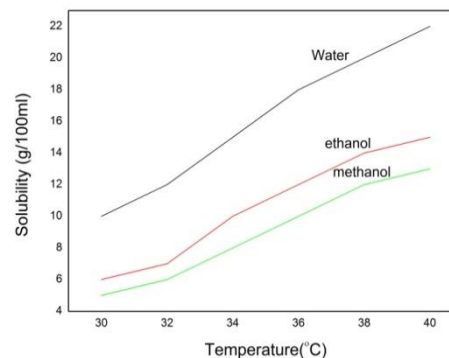


**Figure 1.** Solubility curve of PLAla single crystal

### 2.3 Crystal growth

Single crystals of PLAla was grown by preparing saturated solution in deionized water at room temperature and stirred well to yield a homogeneous mixture of solution. The solution was then filtered thrice to remove the suspended impurities and allowed to evaporate slowly in a constant temperature bath kept at 36 °C, which resulted gradually in supersaturation. Crystals of well optical transparency with the dimensions of 7 mm x 4 mm x 3 mm were harvested. The photograph of as grown single crystal of PLAla is shown in (Figure 2).

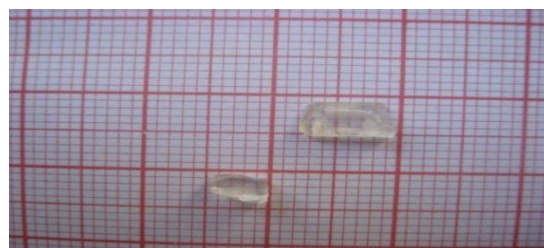


**Figure 2.** Photograph of as grown crystals of Potassium L-alaninate single crystal

## 3. RESULTS AND DISCUSSION

### 3.1 Single crystal X-ray diffraction

The crystals were subjected to X-ray diffraction in an ENRAF Nonius CAD 4 diffractometer with MoK $\alpha$  radiation of  $\lambda = 0.71073 \text{ \AA}$ . The unit cell

parameters are  $a = 6.3 \text{ \AA}$ ,  $b = 7.078 \text{ \AA}$ ,  $c = 15.357 \text{ \AA}$ ,  $\alpha = \beta = \gamma = 90^\circ$ , Volume =  $684.79 \text{ \AA}^3$  with the orthorhombic system of  $P2_12_12_1$  space group.

### 3.2 X-ray Powder diffraction

The X-ray Powder diffraction studies were carried out using powder X-ray diffractometer (P Analytical XPERT PROMPO) with  $\text{CuK}\alpha$  ( $\lambda = 1.5406 \text{ \AA}$ ) radiation. Powder XRD pattern was recorded by scanning the sample over the range  $6^\circ - 60^\circ$  at the rate of  $2^\circ$  per minute. The recorded XRD pattern with hkl indices of PLAla crystals is shown in (Figure 3). The appearance of sharp and strong peaks confirms the good quality of the grown crystals.

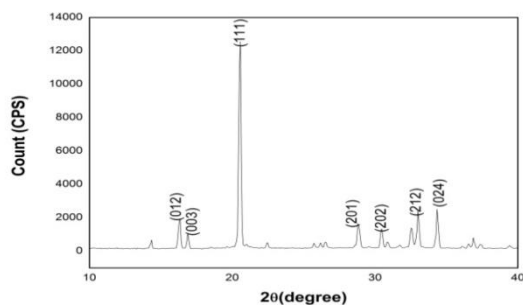


**Figure 3.** XRPD spectrum of PLAla single crystal

### 3.3 UV-vis-NIR spectral analysis

Optical absorption analysis was studied at room temperature by Shimadzu UV-1800 UV-vis-NIR spectrometer. The optical absorption spectrum of PLAla was recorded in the range 190 – 900 nm. Figure 4 ascertains that the crystal has a wide transmission of about 100% in the entire range without any absorption peak. The lower cutoff wavelength of PLAla was found to be 220 nm. The crystal has good optical transmission in the visible region. The transparency in the visible region for the crystal suggests its suitability for second harmonic generation. The measured transmittance (T) was used to calculate the absorption coefficient ( $\alpha$ ) using the relation

$$\alpha = \{2.3026 \log(1/T)\}/t$$

where  $t$  is the thickness of the sample. The optical band gap ( $E_g$ ) is related to optical absorption coefficient ( $\alpha$ ) and energy ( $h\nu$ ) of the incident photon given by [14].

$$\alpha = \{A(h\nu - E_g)^{1/2}\}/h\nu$$

where  $A$  is a constant,  $E_g$  is the optical band gap,  $h$  is the Planck's constant and  $\nu$  is the frequency of the incident photons. The band gap of PLAla crystal was estimated by plotting  $(\alpha h\nu)^2$  versus  $h\nu$  as shown in (Figure 5). From the Figure, the value of band gap was found to be 5.7 eV.

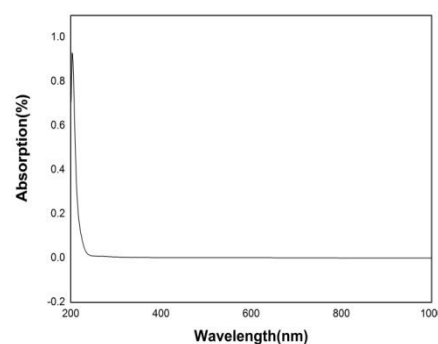


**Figure 4.** Optical absorption spectrum

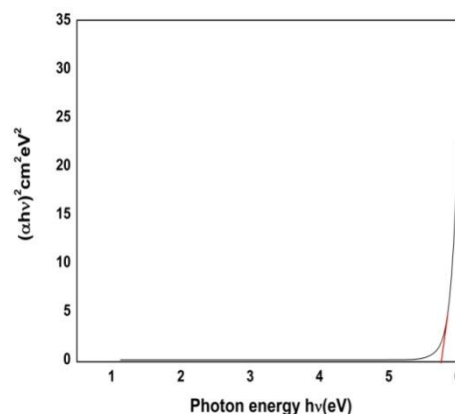


**Figure 5.** Tauc's plot

### 3.4 FTIR spectroscopic analysis

The FTIR spectra of the sample was recorded in the frequency region of  $400 - 4000 \text{ cm}^{-1}$  using PERKIN ELMER RX9 FTIR Spectrometer to

confirm the vibrational structure of the grown crystalline compound. (Figure 6) shows the FTIR spectrum of PLAla. The asymmetric stretching of the  $\text{NH}_3^+$  is observed with wave number  $3085.89 \text{ cm}^{-1}$ . The other vibrational assignments of PLAla single crystals are given in (Table 1).

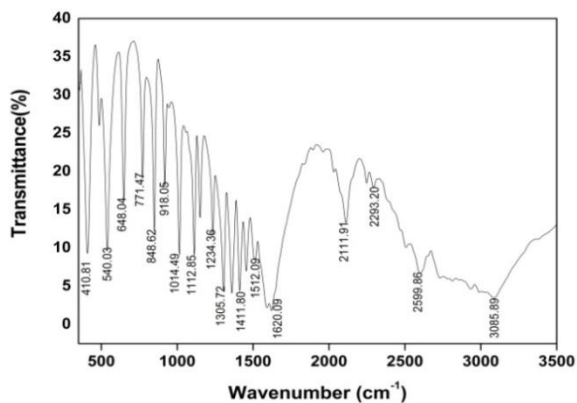


**Figure 6.** FT-IR spectrum of PLAla single crystal

**Table 1.** Vibrational assignments of PLAla crystal

Sl. No	Wavenumber ( $\text{cm}^{-1}$ )	Assignments
1	410.81	Rocking $\text{COO}^-$
2	648.04	$\text{COO}^-$ bending
4	1359.72	C-C stretching
5	1411.80	Symmetric stretching of $\text{COO}^-$
6	848.62	$\text{CH}_3$ bending
7	1512.09	$\text{NH}_3^+$ bending
8	1620.09	Asymmetric bending of $\text{NH}_3^+$

### 3.5 Elemental analysis

To confirm the chemical composition of the synthesized compound, we carried out AAS (Atomic Absorption Spectroscopy) and CHN analysis on the recrystallised sample using the instrument Elementer vario EIII microanalyzer to ascertain the presence of potassium in the as

grown crystals of PLAla. The results of the analysis are presented in (Table 2). Theoretical values of C, H,N and K were found by the molecular formula  $\text{K}^+\text{C}_4\text{H}_8\text{NO}_3$ . The experimental and calculated values of C, H and N agree with each other confirming the formation of PLAla.

**Table 2.** Elemental analysis of PLAla single crystals

Element	Experimental	Calculated
Carbon	34.92	28.57
Hydrogen	5.12	4.76
Nitrogen	11.87	11.11
Potassium	29.23	30.16

### 3.6 TG/DT analysis

Simultaneous thermogravimetry (TG) and differential thermogravimetry analysis (DTA) of powdered sample were performed in the temperature range of  $30 - 600^\circ \text{C}$ , using Seiko Thermal Analyzer a with a heating rate of  $10^\circ \text{C}/\text{min}$ . From TG/DTA curve (Figure 7), only one major loss of weight exists in the TG curve, which might be due to the decomposition of the PLAla single crystal. The decomposition starts at  $230.9^\circ \text{C}$ . There is no phase transition process before  $277.9^\circ \text{C}$ , the crystal is stable up to  $277.9^\circ \text{C}$  which is a higher temperature than for many other semi organic NLO crystals.

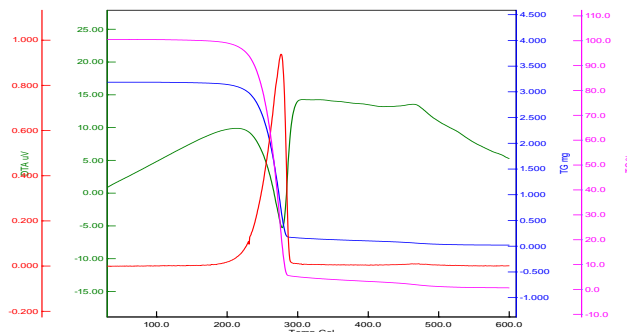


**Figure 7.** TG/DTA curve of PLAla single crystal

### 3.7 Dielectric studies

The dielectric constant and dielectric loss measurements were made using HIOKI 3532 LCR Hitester in the frequency range of 100 Hz – 1MHz. Silver coatings were applied on the opposite sides of the polished crystals and placed between two copper electrodes to form a parallel plate capacitor. The dielectric constant was calculated using the relation

$$\epsilon_r = [A_{air}/A_{cry}] \{C_{cry} - C_{air}(1 - A_{cry}/A_{air})/C_{air}\}$$

Where A is the area of the sample and C is the capacitance of the crystal. The observations were made while cooling the sample in the frequency range 20 Hz to 1 MHz at the temperature of 50 to 150°C. Figure 8 and Figure 9 shows the plot of dielectric constant ( $\epsilon_r$ ) as a function of frequency and dielectric loss (D) as a function of log frequency respectively. It is observed that the  $\epsilon_r$  and D both are inversely proportional to the frequency. This is a normal dielectric behaviour [15] that both  $\epsilon_r$  and D decrease with increasing frequency. This can be understood on the basis of the mechanism of polarization which is similar to that of conduction process. The electronic exchange of the number of ions in the crystal gives local displacement of electrons in the direction of the applied field which in turn gives rise to polarization [16]. It is seen from the Figure 8, that the dielectric constant has higher values in the lower frequency region and then it decreases with the applied frequency. The very high value of  $\epsilon_r$  and low frequencies may be due to the presence of all the four polarization namely space charge, orientational, electronic and ionic polarization and it's low value of at higher frequencies might be due to the loss of significance of these polarization gradually [17]. Dielectric loss is also studied as a function of frequency at various temperatures and it is shown in (Figure 9). These curves suggest that the dielectric loss strongly depends on the frequency of the applied field, similar to that of dielectric constant. This behaviour is common in the case

of ionic system also [18-19]. The low value of dielectric loss indicates that the grown crystals are of good quality free from defects.

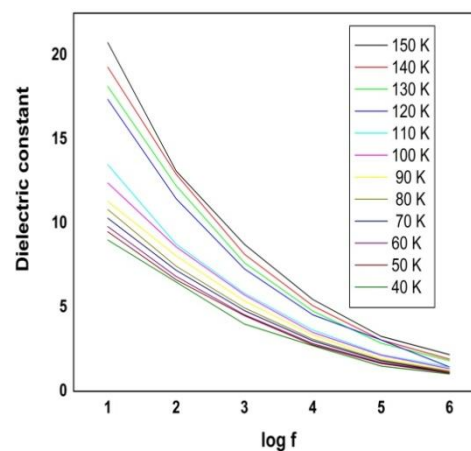


Figure 8. Variation of dielectric constant

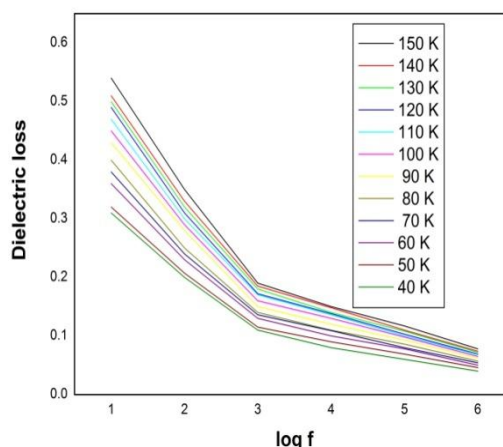


Figure 9. Variation of dielectric loss

### 3.8 AC conductivity studies

The AC conductivity studies of PLAla single crystal was performed using a LCR meter in a temperature range from 50-150°C. The AC conductivity graph is shown in Figure 10. It is seen from the graph that the conductivity increases when the temperature increases. Therefore defects concentration increases when the temperature rises. At higher frequencies, the increased conductivity is due to the reduction in the space charge polarization. As seen from the

dielectric graph, it may be interpreted that the dielectric constant of the dispersive medium decreases because the term contributing to dielectric constant from ion-dipole- interaction is compensated by the thermal energy leading to the relaxation of polarization [20]. Hence an increase in conductivity at higher frequencies for a given temperature confirms small polaron hopping in the crystal [21]. The AC conductivity of PLAla single crystal increases on increasing the frequency. The electrical conduction in dielectrics is mainly a defect controlled process in the low temperature region.

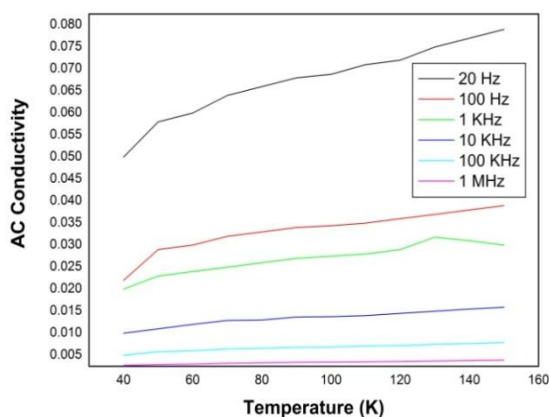


Figure 10. Variation of ac conductivity

### 3.9 Microhardness Studies

Microhardness measurements were done using a Vickers’s microhardness indenter using Leitz Weitzier Hardness Tester. The indentation time was fixed as 10 s. The mechanical properties of the grown crystal was also studied. The applied loads are 25, 50 and 100 g and hardness was calculated using the relation

$$H_v = 1.8554 \frac{P}{d^2} \text{ Kg mm}^{-2}$$

Where P is the load applied in kg and d is the diagonal length of the indented impressions in mm. A plot between load P and hardness number  $H_v$  is shown in (Figure 11), which shows that the microhardness number

increases with increasing load for the grown crystal. The graph between  $\log P$  Vs  $\log d$  for PLAla crystals are shown in (Figure 12). The slope of the straight line gives the work hardening coefficient (n). The value for the work hardening coefficient for PLAla crystal was found to be 2.67. According to Onitsch [22], if n is greater than 1.6, the crystal belongs to soft category. As n is less than 1.6, it can be said that PLAla crystal belongs to soft material category.

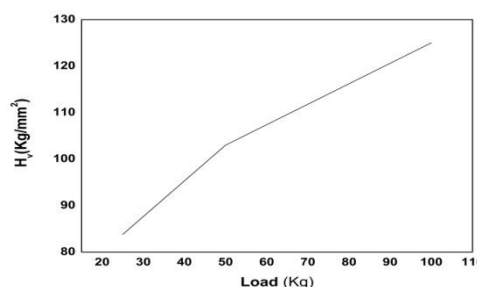


Figure 11. Vickers hardness number

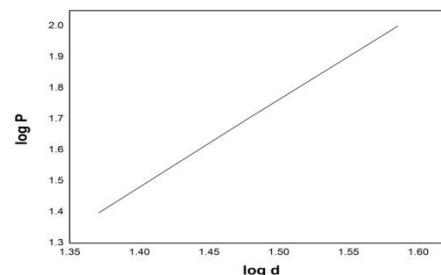


Figure 12. Plot between log P and log d

### 3.10 NLO Test

The SHG behaviour of the powdered material was tested using Kurtz and Perry method [23]. The sample was ground into a very fine powder and tightly packed in a micro capillary tube. Then it was mounted in the path of Nd:YAG laser beam of 9.6 mJ/pulse energy obtained by splitting the original laser beam. The output light was passed through a monochromator which detected the green light at 532 nm. This confirms the NLO behavior of the material. The green light intensity was registered by a photomultiplier tube and

converted into an electrical signal. This signal was displayed on the oscilloscope screen. The sample was replaced by potassium dihydrogen ortho phosphate (KDP) and the signal was displayed in the oscilloscope screen. SHG conversion efficiency was computed by the ratio of signal amplitude of the PLAla crystal to that of the KDP signal amplitude recorded for the same input power. The SHG relative efficiency of PLAla crystal was found to be 1.2 times higher than that of KDP.

## CONCLUSION

A new nonlinear semi organic SONLO crystal PLAla was successfully grown employing slow solvent evaporation technique. A convenient size of 7 mm x 4 mm x 3 mm was harvested in a month time. The solubility of PLAla single crystal was estimated to be 17 g in 100ml of water at room temperature. The various functional groups in PLAla crystal was identified using FTIR analysis. The UV-VIS- NIR spectral analysis showed good transparency in the UV and visible region. The dielectric constant and dielectric loss measurements of PLAla crystal revealed the normal behavior. AC conductivity studies performed on PLAla single crystal establishes the mechanism of polarization. The SHG relative efficiency of PLAla single crystal was found to be 1.8 times higher than that of KDP.

## REFERENCES

1. Meenakshisundaram, S.; Parthiban, S.; Bhagavannarayana, G.; Madhurambal, G.; Mojumdar, S. C.; Influence of organic solvent on thiristiourea zinc(II)sulphate crystals. *Journal of Thermal Analysis and Calorimetry* 2009, 96, 125-129.
2. Shirsat, M. D.; Hussaini, S. S.; Dhumane, N. R.; Dongre, V. G. Influence of lithium ions on the NLO properties of KDP single crystals. *Crystal Research Technology* 2008, 43 (7), 756-761.
3. Hussaini, S. S.; Dhumane, N. R.; Dongre, V. G. Karmuse, P. Ghughare, P.; Shirsat, M. D. Effect of glycine on the optical properties of Zinc Thiourea chloride (ZTC) single crystal, *Journal of Optoelectronics and Advanced Materials - Rapid Communication* 2008, 2, 108.
4. Meera, K.; Muralidharan, R.; Dhanasekaran, R.; Manyum Prapun; Ramasamy, P. Growth of nonlinear optical material: L-arginine hydrochloride and its characterisation. *Journal of Crystal Growth* 2004, 263, 510-516.
5. Misoguti, L et al. Optical properties of L-alanine organic crystals. *Optical Materials* (1996), 6, 147-152.
6. Jaikumar, D.; Kalainathan, S.; Bhagavanarayana, G. Synthesis, growth, thermal, optical and mechanical properties of new organic NLO crystal: L-alanine DL-malic acid. *Journal of Crystal Growth* 2009, 312, 120-124.
7. Lydia Caroline, M.; Vasudevan, S. Growth and characterization of an organic nonlinear optical material: L-alanine alaninium nitrate. *Materials Letters* 2007.
8. Ramachandra Raja, C.; Antony Joseph, A. Crystal growth and characterization of new nonlinear optical single crystals of L-alaninium fumarate. *Materials Letters* 2009, 63, 2507-2509.
9. Mohan Kumar, R. et al. Studies of growth aspects of semi-organic L-alanine acetate: a promising NLO crystal. *Journal of Crystal Growth* 2005, 275, 1935-1939.
10. Justin Raj, C. et al. Studies on optical, mechanical and transport properties of NLO active L-alanine formate single crystal grown by modified Sankaranarayanan-Ramasamy (SR) method. *Optics Communications* 2008, 281, 2285-2290.

11. Krishnakumar, V.; Nagalakshmi, R. Polarised Raman and infrared spectral analysis of L-alanine oxalate- a non-linear optical single crystal. *Spectrochimica Acta Part A* 2006, 64,736-743.
12. Jaikumar, D. et al. Structural, spectral, thermal, dielectric, mechanical and optical properties of Urea L-alanine acetate single crystals, *Physica B* 2010,405, 2394-2400.
13. Rajan Babu, D. et al. Growth and characterization of non-linear optical L-alanine tetrafluoroborate single crystals, *Journal of Crystal Growth* 2002, 245, 121-125 .
14. Ashour, A.; El-Kadry, N.; Mahmoud, S.A. On the electrical and optical properties of CdS films thermally deposited by a modified source, *Thin Solid Films* 1995, 269, 117–120
15. Anderson, Dielectrics, J. C. Chapman and Hall, London, 1964
16. Senthil Murugan, G.; Ramasamy, P. Growth and characterization of metal-organic crystal: Tetra thiourea cobalt chloride (TTCOC), *Journal of Crystal Growth* 2009, 311 (3), 585-588.
17. Ambujam, K.; Thomas, P. C.; Aruna, S.; Prem Anand, D.; Sagayaraj, P. Growth and Characterization of dichloro tetrakis thiourea nickel single crystals. *Crystal Research Technology* 2006, 41, 1082-1088.
18. Rao, K.V.; Smakula, A. Dielectric Properties of Cobalt Oxide, Nickel Oxide and Their Mixed Crystals. *Journal of Applied Physics* 1965, 36 (6) 2031-2038.
19. Rao, K.V.; Smakula, A. Dielectric Properties of Alkaline Earth Fluoride Single Crystals. *Journal of Applied Physics* 1966, 37(1), 319-323.
20. Smyth, C.P. Dielectric behavior and structure. McGraw-Hill, New York 1955.
21. Austin, I.G.; Mott, N.F. Polarons in crystalline and non-crystalline materials. *Advanced Physics* 1969, 18, 41-102
22. Krishnan, C.; Selvarajan, P.; Pari, S. Synthesis, growth and studies of undoped and sodium chloride –doped Zinc Tris-thiourea Sulphate (ZTS) single crystals. *Current Applied Physics* 2010, 10, 664.
23. Kurtz, S.K.; Perry, T.T. A Powder technique for the Evaluation of Nonlinear Optical Materials. *Journal of Applied Physics* 1968, 39, 3798- 3813.

#### AUTHOR PROFILE



**Dr. D. Prem Anand** received M.Sc., M.Phil and Ph.D in physics from Madras University. He has been actively doing research from 2004. He has published many research articles in national and international journal. He is working in the field of crystal growth and nanotechnology. He is an assistant professor of physics at St. Xavier's College, Palayamkottai.



**S. Anna Venus** received **M.Phil** in Physics from Madurai Kamarajar University. She is working as an assistant professor of Physics in St. Xavier's College, Palayamkottai and doing Ph.D under the guidance of Dr. D. Prem Anand in the field of crystal growth and characterization.